

# BPW34 Commercial *p-i-n* Diodes for High-level 1-MeV Neutron Equivalent Fluence Monitoring

Federico Ravotti, *Member, IEEE*, Maurice Glaser, Michael Moll and Frédéric Saigné

**Abstract**—The BPW34 *p-i-n* diode was characterized at CERN in view of its utilization as radiation monitor at the LHC to cover the broad 1-MeV neutron equivalent fluence ( $\Phi_{eq}$ ) range expected for the LHC machine and experiments during operation. Electrical measurements for both forward and reverse bias were used to characterize the device and to understand its behavior under irradiation. When the device is powered forward, a sensitivity to fast hadrons for  $\Phi_{eq} > 2 \times 10^{12} \text{ cm}^{-2}$  has been observed. With increasing particle fluences the forward I-V characteristics of the diode shifts towards higher voltages. At  $\Phi_{eq} > 3 \times 10^{13} \text{ cm}^{-2}$ , the forward characteristic starts to bend back assuming a thyristor-like behavior. An explanation for this phenomenon is given in this article. Finally, detailed radiation-response curves for the forward bias-operation and annealing studies of the diode's forward voltage are presented for proton, neutron and gamma irradiation.

**Index Terms**—Radiation monitoring, *p-i-n* diodes, accelerators, particle beams, radiation damage.

## I. INTRODUCTION

THE particle fluence expected over 10-years in the Experiments of the LHC accelerator at CERN [1] will cover a broad range of more than five orders of magnitude from  $10^8\text{-}10^{10}$  to  $10^{14}\text{-}10^{15}$  particle/cm<sup>2</sup> depending on the position in the Experiment. While for lower fluence ranges dosimeter diodes exist [2], they couldn't be employed to monitor 1-MeV neutron equivalent fluences ( $\Phi_{eq}$ ) higher than a few  $10^{12} \text{ cm}^{-2}$ . For this reason BPW34 *p-i-n* diodes have been studied in order to evaluate their performances as high-level particle fluence monitor. Moreover, the fact that these devices are commercially available in large numbers at a relatively low cost makes the possibility of using them as fast-hadron dosimeter an attractive prospect.

According to the concept of the Non Ionizing Energy Loss (NIEL) Hypothesis the radiation induced bulk damage in semiconductor devices can be scaled by the non-ionizing energy transfer to the lattice of the semiconductor crystal. In

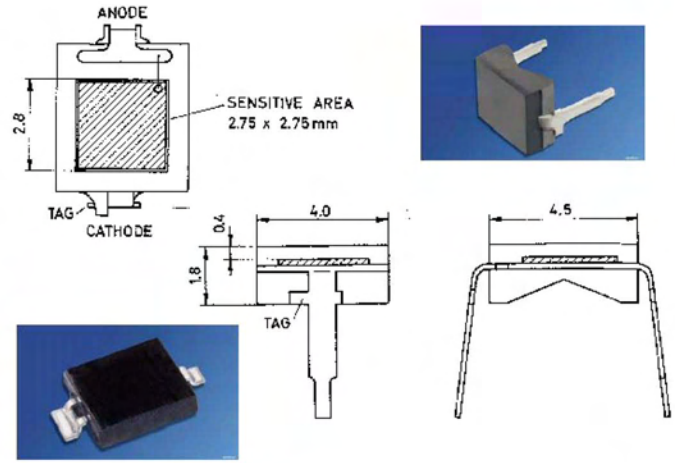


Fig. 1. The layout of the *p-i-n* diodes BPW34F as commercially supplied in DIL (top right-hand corner) and SMD packages (bottom left-hand corner).

this work we use the definition of NIEL and scaling factors (hardness factors  $\kappa$ ) as defined in [3].

The BPW34 *p-i-n* diodes are devices produced by several semiconductor companies. Their applications are mainly in the field of photo-interrupters and IR remote controls. A list of typical electrical and optical characteristics for this device can be found in [4]. According to the electronic nomenclature, the part number BPW34 means the following: B is the material used for the active region of the device (B = silicon), P indicates the circuit function (P = radiation sensitive diode) and W34 is the serial number.

As shown in Fig. 1 the diode consists of a small  $2.75 \times 2.75 \text{ mm}^2$  silicon die (the active part of the component) encased in a plastic packaging which allows an easy handling. This component is available in two different DIL packages:

- BPW34: transparent plastic packaging that allows the device to be sensitive to light from 400 nm to 1100 nm;
- BPW34F: plastic packaging with a daylight filter limiting the light sensitivity of the device to about 950 nm to 1100 nm (see right-hand side of Fig. 1).

Because of their lower sensitivity to light, all samples used for this study were packaged diodes of the type BPW34F.

Manuscript received September 7, 2007.

F. Ravotti and F. Saigné are with IES – UMR UMII-CNRS 5214, University Montpellier II, Place E. Bataillon, c.c. 083, F-34095, Montpellier Cedex 5, France. F. Ravotti is also with Physics Department, CERN, Geneva 23, CH-1211, Switzerland (e-mail: Federico.Ravotti@cern.ch).

M. Glaser and M. Moll are with Physics Department, CERN, Geneva 23, CH-1211, Switzerland (Maurice.Glaser@cern.ch).

This *p-i-n* diode is also supplied in SMD plastic packaging as shown in the left-hand side insert of Fig. 1.

## II. PRELIMINARY STUDIES AND UNDERSTANDING OF THE DEVICE RADIATION RESPONSE

### A. Conclusions from previous studies

The first study of the BPW34F diode (produced by SIEMENS) as neutron sensor was addressed at CERN in 1992. The results of irradiation tests in the neutron field of the PSAIF facility [5] at CERN were summarized in a CERN Report from Malfante [6] and were the following:

1. The devices are reported to have a base thickness (*W*) of 210  $\mu\text{m}$  and a resistivity of 2.5  $\text{k}\Omega\cdot\text{cm}$ ;
2. The dosimetric signal  $V_F$  (forward voltage) were measured, after irradiation, in condition of intermediate injection (1 mA) with constant forward current;
3. The response of the diodes to neutrons was sometimes far from linear: the measured sensitivity to neutrons ( $E > 140 \text{ keV}$ ) was about  $35\text{-}50 \text{ mV}/10^{12} \text{ cm}^{-2}$ . The lower particle fluence measured in the Malfante study was around  $10^{12} \text{ cm}^{-2}$ . No clear information about the diodes behavior at lower neutron fluence was given;
4. Irradiations with  $\gamma$ -rays were performed on these diodes and their response was found to be very low compared to the neutron response. For 100 kGy of ionizing dose, a  $\Delta V_F$  of about 100 mV was measured;
5. Following a neutron irradiation of  $\Phi_{(>140 \text{ keV})} = 2.5 \times 10^{13} \text{ cm}^{-2}$  a room temperature annealing of  $V_F$  of about 0.5 % was measured after 21 days.

### B. Forward bias on-line vs. off-line radiation responses

Several irradiation campaigns were carried out exposing the BPW34F diodes to the 23 GeV proton beam of the IRRAD1 facility and to the neutron environment of the IRRAD2 facility at CERN [7]. All samples irradiated in this work have been exposed to the different particle beams with the terminals shorted to ground. A summary of these preliminary results is given in Fig. 2, where the measurements performed during radiation exposure (on-line) are plotted as function of  $\Phi_{\text{eq}}$  for the two facilities. To allow a comparison of the IRRAD1 data with the results obtained in the IRRAD2 facility, the proton fluence was converted into  $\Phi_{\text{eq}}$  by means of the experimentally determined hardness factor of 0.62 [8]. At the irradiation position in IRRAD2 the hardness factor, calculated using the facility spectra, is 0.67 [9].

The on-line data, plotted with triangular markers, are an average of different irradiation tests performed at proton fluxes ranging from  $1.1 \times 10^8$  to  $1.1 \times 10^{10}$  protons/( $\text{cm}^2\cdot\text{s}$ ) while the neutron ones were obtained at a 1-MeV neutron equivalent flux of  $8.3 \times 10^7 \text{ cm}^{-2}\cdot\text{s}^{-1}$ . All  $V_F$  measurements were carried out at intermediate injection level (1 mA) with a forward current pulse ranging from 100 ms to 700 ms duration. In this condition no significant differences regarding the response of the devices to the two different types of particles were observed.

Both data sets follow the same trend. After an initial “flat” region up to  $\Phi_{\text{eq}}$  of  $2 \times 10^{12} \text{ cm}^{-2}$ , in which the particle sensitivity appears to be slightly negative (a few tens of mV not visible in the log plot of Fig. 2), the response is linear of the type  $\Delta V_F = c \cdot \Phi_{\text{eq}}$  up to several  $10^{14} \text{ cm}^{-2}$ . In this equation  $c$  represents the calibration coefficient of the diode. Thus this relationship is in agreement with the concept of the NIEL Hypothesis, which claims that the generation of silicon bulk damage is scaling with the non-ionizing energy transfer to the lattice [3]. These results prove that this device is suitable to measure high particle fluences. A  $V_F$  of about 1-2 V was measured for a  $\Phi_{\text{eq}}$  of  $1 \times 10^{13} \text{ cm}^{-2}$ . Taking into account the difference in the readout methods and in the particle spectra, this sensitivity is in fairly good agreement with the values measured earlier by Malfante (see Sec. II.A).

In Fig. 2, the on-line measurements are compared with a series of data taken immediately after irradiation (off-line) without performing any annealing procedure before their readout. While the on-line data represent the  $V_F$  increase from the same device, the off-line measurements were obtained using different samples exposed to different particle fluences. For the off-line data presented in Fig. 2 the initial distribution of  $V_F$  was unknown. Nevertheless, the agreement of the unannealed data lies around  $\pm 30\%$ .

In parallel with the tests presented in Fig. 2, a series of room temperature annealing measurements were performed. Following a proton irradiation of  $1.2 \times 10^{14} \text{ cm}^{-2}$ , the tested devices showed a decrease in  $V_F$  of more than 20% after 300 hours. This result thus revealed that long-term annealing phenomena can be an issue for the precision achievable in the particle fluence measurements with this kind of device.

### C. Radiation response mechanism

The radiation response behavior of the forward-biased diodes shown in Fig. 2 agrees with what was theoretically predicted by Swartz and Thurston [10] for a low-resistivity, small W/L (width of the diode base over diffusion length)

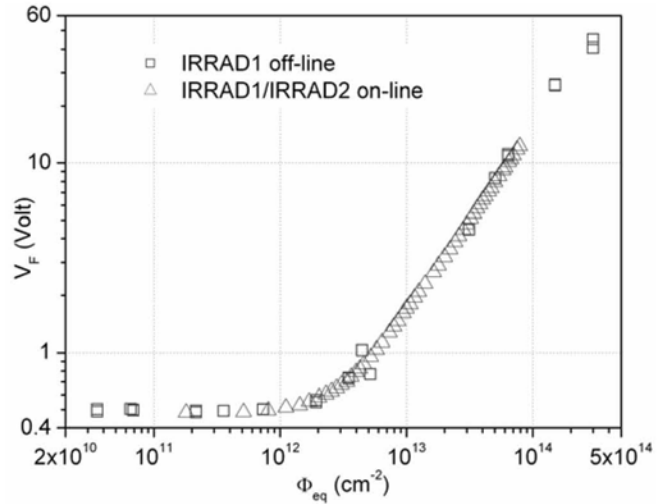


Fig. 2. BPW34F on-line vs. off-line measurements at the IRRAD1 and IRRAD2 facilities at CERN.

ratio, *p-i-n* diode operating at intermediate injection level. According to Ref. [10], the forward voltage  $V_F$  is a sum of the voltage drop at the *p-i* and *i-n* junctions together with the voltage drop over the intrinsic base. Since, for the BPW34F diode, initially  $L$  is essentially larger than  $W$ , the forward voltage across the diode starts to decrease under irradiation due to the predominant decrease of the junction voltages caused by the decrease of the minority carrier lifetime. Increasing the irradiation level, the overall voltage sensitivity to particles becomes then positive due to the reduction of  $L$  to lengths of the order of  $W$  (i.e. increase of

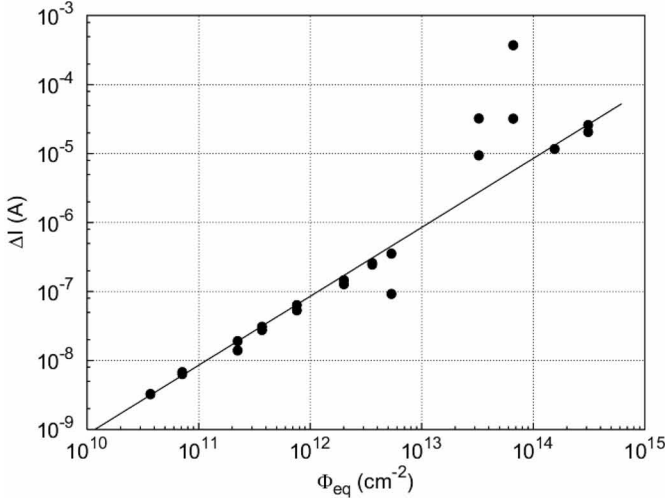


Fig. 3. BPW34F characteristics in reverse bias normalized to 20°C. Leakage current measurement and increasing irradiation levels with 23 GeV protons.

junction voltages). At high irradiation levels, the increases of the base resistance (i.e. increases of base voltage) also start to contribute to the total  $V_F$  increase [11].

### III. DEVICE CHARACTERIZATION

For the following studies, the devices tested were procured from different sensor batches produced by OSRAM [4] in different production sites and time periods. Before starting a systematic study of the BPW34F sensor, a batch of 145 diodes was characterized in order to ensure the homogeneity of the Devices Under Test (DUT). Therefore, for each sample, the  $V_F$  under 1 mA constant current injection was measured at a temperature of  $23.5 \pm 1.7^\circ\text{C}$ . From this preliminary screening, a group of specimens homogeneous within  $\pm 11\%$  and with an average  $V_F$  of 0.531 V was selected.

#### A. Reverse bias measurements

After several steps of proton irradiation in the IRRAD1 facility, the determination of the diode leakage current has been done by means of I-V and C-V measurements. The radiation-induced increase of the leakage current  $\Delta I$  is given by the difference between the current measured after and before irradiation. In Fig. 3 the leakage current increase of the BPW34F diodes has been plotted vs.  $\Phi_{\text{eq}}$  after being normalized to 20°C.

In the picture, each point corresponds to an individual diode

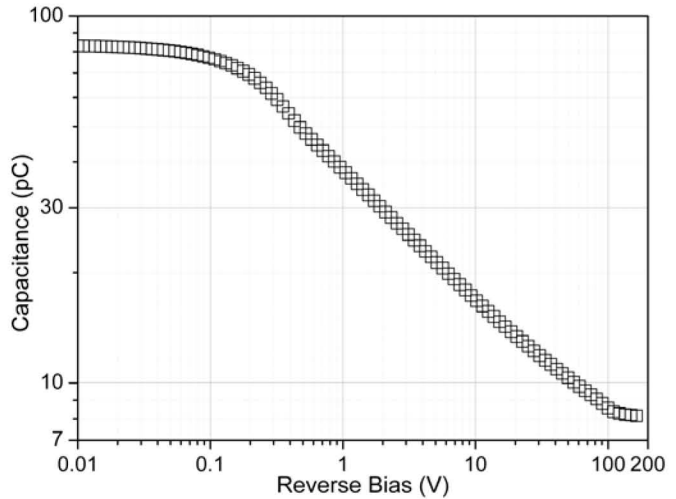


Fig. 4. Capacitance measurement for an un-irradiated BPW34F diode.

irradiated with protons in a single exposure to a given fluence. Moreover, before measurement the individual samples were brought to the same annealing state by heating them for 4 minutes to  $80^\circ\text{C}$ . The chosen annealing cycle has been selected in agreement with the standard procedure adopted to anneal silicon particle detector structures [12]. From Fig. 3 it is possible to see that the leakage current increase is proportional to  $\Phi_{\text{eq}}$  in the range from  $10^{10} \text{ cm}^{-2}$  to  $10^{13} \text{ cm}^{-2}$ . After this point, the measured  $\Delta I$  was much higher with respect to the foreseen linear behavior. A similar result has also been found for a second series of diodes irradiated with neutrons at the IRRAD2 Facility. For  $\Phi_{\text{eq}} < 10^{13} \text{ cm}^{-2}$ , the diodes can thus be used as NIEL counter in the same way as the particle detector diodes presented in [2].

#### B. Measurement of base thickness and material resistivity

The data of Fig. 3 for  $\Phi_{\text{eq}} < 10^{13} \text{ cm}^{-2}$  were linearly fitted (continuous line in the picture) and the proportionality factor  $\Delta I/\Phi_{\text{eq}}$  was calculated to be  $5.17 \times 10^{-20} \text{ A} \cdot \text{cm}^2$ . The above data can be conveniently used for a first estimate of the base

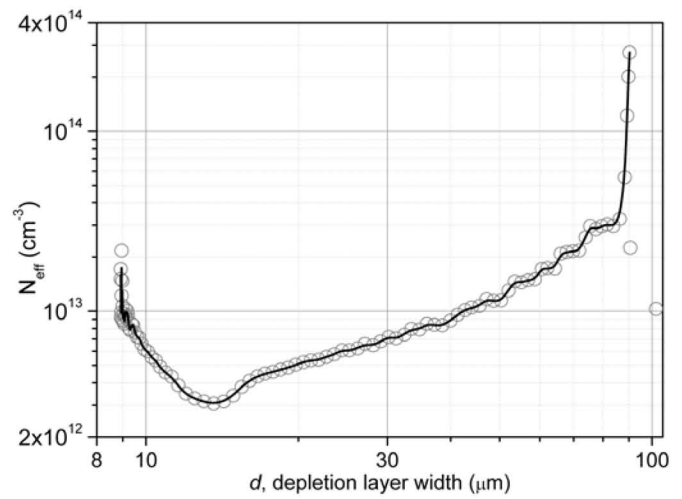


Fig. 5. Doping profile (effective doping concentration vs. depletion layer width) of the BPW34F diode extracted from the capacitance measurement of one non-irradiated sample.

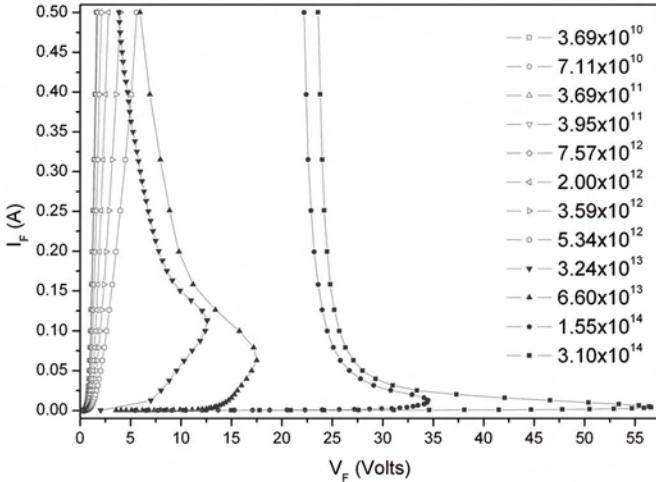


Fig. 6. Forward I-V curves after 23 GeV proton irradiations (linear scale). In the y-axis the current (A) upon 100 ms wide forward voltage bias pulses is plotted. Each curve corresponds to a different  $\Phi_{eq}$  as indicated in the legend.

thickness ( $W$ ) of the BPW34F device by comparing it with the current related damage rate ( $\alpha$ ) measured from a calibrated series of particle detector diodes [2] irradiated at the same time of the DUT. Once the value of  $W$  is known, it is possible to estimate the material resistivity by using the depletion voltage measured on a non-irradiated diode (see C/V measurement of Fig. 4). Details about this calculation can be found in [13]. With this method a  $W$  of about 300  $\mu\text{m}$  and an average material resistivity of 2.7  $\text{k}\Omega \cdot \text{cm}$  were estimated.

In order to give a comprehensive evaluation, we want to approach here the above calculations also in a different way using a different method. The C/V curve of a non irradiated diode shown in Fig. 4 allows, via Eq. 1, the extraction of the diode's doping-profile [14].

$$N_{eff}(d) = \frac{2}{A^2 \epsilon \epsilon_0 q} \left( \frac{d(1/C^2)}{dV} \right)^{-1} \quad (1)$$

In Eq. 1,  $\epsilon_0 = 8.85 \times 10^{-14} \text{ F/cm}$ ,  $\epsilon = 11.9$  for silicon,  $A$  is the area of the device ( $0.0702 \text{ cm}^2$ ) and  $q$ , the elementary charge, is equal to  $1.602 \times 10^{-19} \text{ C}$ . In this equation  $d$  indicates the

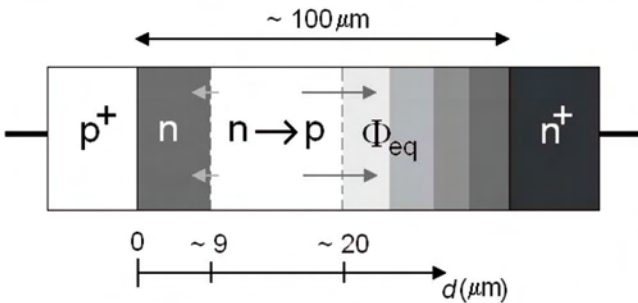


Fig. 7. Mechanism of formation of  $p-n-p-n$  thyristor structures in heavily irradiated forward biased BPW34F  $p-i-n$  diodes. Due to the in-homogeneity of  $N_{eff}$ , the region of the intrinsic n-type Si base at  $9 < d < 20 \mu\text{m}$  start to type-invert at  $\Phi_{eq}$  of about  $3 \times 10^{13} \text{ cm}^{-2}$  leading to the formation of the  $p-n-p-n$  double junction structure. Drawing is not in scale.

width of the depletion layer that is related to the measured capacitance  $C(V)$  via Eq. 2:

$$C(V) = \frac{\epsilon \epsilon_0 A}{d(V)} \quad (2)$$

As visible in Fig. 4, with increasing voltage the capacitance decreases and reaches with full depletion a final value when  $d$  become equal to the base thickness of the diode ( $W$ ).

Fig. 5 shows a clearly non-homogeneous doping profile of the silicon base with a minimum  $N_{eff,min}$  of  $3 \times 10^{12} \text{ cm}^{-3}$  in the region of  $d$  comprised from 9 to 20  $\mu\text{m}$ . From Fig. 5 it is also possible to evaluate the base-thickness of the BPW34F device to about 100  $\mu\text{m}$ . By averaging the  $N_{eff}(d)$  plotted in Fig. 5, and knowing the electron mobility in n-type silicon ( $\mu_n = 1450 \text{ cm}^2 \cdot \text{V}^{-1} \cdot \text{s}^{-1}$ ), it is finally possible to evaluate the material resistivity:

$$\rho = \frac{1}{q \mu_n N_{eff}} \approx 0.5 - 1 \text{ k}\Omega \cdot \text{cm} \quad (3)$$

The above values of  $W$  and  $\rho$  (obtained with two different experimental techniques) and the ones from bibliographic data (see Sec. II.A) lie within a factor 3.

Nevertheless, all these results confirm that the DUT is a relatively low-resistivity, small  $W$ ,  $p-i-n$  diode with a forward bias radiation response that can be described with the mechanism summarized in Sec. II.C.

#### IV. STUDY OF THE FORWARD BIAS RADIATION RESPONSE

The characterization of the BPW34F diodes in forward bias has been done by measuring the forward I-V curves for samples irradiated to different  $\Phi_{eq}$  levels with 23 GeV protons and in the neutron field of IRRAD2 at CERN. A total of 24 diodes were exposed to protons and another 20 to neutrons. For a given fluence step, two devices were exposed in order to get redundancy in the results. The measurements were carried out after irradiation, using a test-bench based on a stand-alone Keithley 2400, injecting increasing 100 ms-wide current pulses and recording the corresponding forward voltages across the device terminals. All experiments were carried out in a light-tight box. Fig. 6 displays the results of the measurements following proton irradiation. Each curve corresponds to the average of the two I-V curves measured for devices exposed at the same time. For  $\Phi_{eq} < 1 \times 10^{13} \text{ cm}^{-2}$  the I-V curve of the diode shifts in the positive direction with increasing particle fluence. At higher fluences the curves start to bend back towards smaller  $V_F$  when forward currents in the order of 100 mA are reached. From that point onwards the BPW34F I-V assumes a thyristor-like behavior. The set of devices irradiated with neutrons in IRRAD2 exhibit the same thyristor-like behavior for  $\Phi_{eq}$  exceeding  $1 \times 10^{13} \text{ cm}^{-2}$ .

It has been reported in the literature [15] that radiation induced changes in silicon conductivity can lead to the formation of  $p-n-p-n$  thyristor structures in devices powered in forward bias as in the case of the DUT. The doping profile of

the BPW34F diode calculated in Fig. 5 allows us to propose an explanation of this observed behavior.

It is known from particle detector irradiation studies [16] that the conduction-type inversion point in silicon is sensitive to the initial resistivity and thus to the initial effective impurity concentration of the silicon material. 1-MeV neutron equivalent fluences of about  $3\text{-}6 \times 10^{13} \text{ cm}^{-2}$  had been shown to be responsible for the type-inversion of silicon detectors with initial  $N_{\text{eff}} \sim 2\text{-}3 \times 10^{12} \text{ cm}^{-3}$  [17]. According to Fig. 5, the non-uniform doping-profile of the BPW34F diode reaches its minimum ( $N_{\text{eff,min}}$ ) in the base region comprised from 9 to 20  $\mu\text{m}$ . Therefore, as schematized in Fig. 7, is in this region that the change in the conduction-type of the diode begins at a  $\Phi_{\text{eq}}$  of about  $3 \times 10^{13} \text{ cm}^{-2}$ , leading to the formation of a  $p\text{-}n\text{-}p\text{-}n$  double junction structure. Compared to the dimensions of a typical parasitic thyristor structure encountered in CMOS or IGBT, the 9  $\mu\text{m}$  n-type region left is large enough to observe a thyristor like behavior [18]. At higher  $\Phi_{\text{eq}}$  levels the inverted region extends further following the smooth increase of  $N_{\text{eff}}$  for increasing  $d$ , so that for  $\Phi_{\text{eq}} \sim 1 \times 10^{14} \text{ cm}^{-2}$ , the  $p\text{-}n\text{-}p\text{-}n$  junction is well established, as shown in the curves of Fig. 6.

From a more practical point of view, thanks to the above observations it is possible to define 25 mA as the upper limit for the injected forward current with which the BPW34F diode can be used in dosimetric applications before entering in thyristor regime.

Taking into account all the above measured curves, the values of  $V_F$  as function of  $\Phi_{\text{eq}}$  have been extracted for three selected currents in order to determine the variation of the hadron sensitivity at different forward currents. The three selected currents were 1 mA (usual readout current), 25 mA

TABLE I  
BPW34F HADRON SENSITIVITY AT DIFFERENT INJECTION-LEVELS

Forward current (mA)	$1/c$ ( $\text{cm}^2/\text{mV}$ )	Sensitivity increases (%)	Upper limit linear-range $\Phi_{\text{eq}} (\text{cm}^{-2})$
1	$9.1 \times 10^9$	-	$\geq 4 \times 10^{14}$
10	$1.04 \times 10^{10}$	14	$< 2 \times 10^{14}$
25	$1.24 \times 10^{10}$	36	$< 1 \times 10^{14}$

(maximum level allowed from the observation of the I-V behaviors) and 10 mA. This last value has been intentionally selected in between the previous two according to the electronic standards for commercial current sources. Following the theoretical indications of [10], the radiation response of forward biased  $p\text{-}i\text{-}n$  diodes to particle irradiation is expected to be improved at higher injection levels. For this reason, forward currents lower than 1 mA have not been considered here. For  $\Phi_{\text{eq}} < 2 \times 10^{12} \text{ cm}^{-2}$ , independently on the forward current used, the devices don't show sensitivity to fast hadrons.

As reported in Table I, for  $\Phi_{\text{eq}} > 2 \times 10^{12} \text{ cm}^{-2}$ , the linear part of the characteristics has been used to determine the sensitivity increase at 10 and 25 mA with respect to the one determined at 1 mA. The diode calibration factor is defined as the inverse of the coefficient  $c$  that describes the growth of  $V_F$

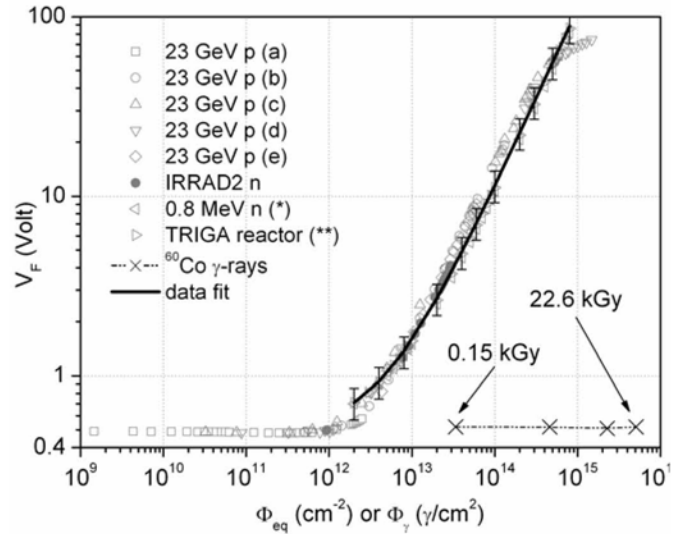


Fig. 8. Radiation response of BPW34F diodes at room temperature. The diode's forward voltage at 1 mA is plotted versus the  $\Phi_{\text{eq}}$ . The width of the readout current pulse was of 700 ms. The experimental data taken in IRRAD1 at CERN has been recorded at different proton rates: (a)  $2.4 \times 10^{11} \text{ cm}^{-2}\text{-h}^{-1}$ , (b)  $3.7 \times 10^{12} \text{ cm}^{-2}\text{-h}^{-1}$ , (c)  $8.1 \times 10^{12} \text{ cm}^{-2}\text{-h}^{-1}$ , (d)  $2.0 \times 10^{13} \text{ cm}^{-2}\text{-h}^{-1}$ , (e)  $2.5 \times 10^{13} \text{ cm}^{-2}\text{-h}^{-1}$ . In the same pictures data from Ref. [21] (\*), Ref. [22] (\*\*) and following exposure to  $\gamma$ -rays have been also reported. For the photon data, the x-axis corresponds to the number of photons per square centimetres. Error bars of  $\pm 20\%$  have been reported to show the accuracy of the data best-fit.

with  $\Phi_{\text{eq}} (I/c)$ . At 25 mA the gain in sensitivity is 36%. However, under this high injection conditions, the dynamic range is reduced by about a factor 4. Although the readout current can be chosen by the user to select the device sensitivity, from the presented results it appears that 1 mA remains the readout condition that insures the best compromise between the achieved sensitivity and the measurable fluence range.

Studies of the time structure of the signal (i.e.  $V_F$  as function of time after current pulse injection) of irradiated BPW34F diodes have been carried out on samples irradiated up to  $\Phi_{\text{eq}} = 1 \times 10^{14} \text{ cm}^{-2}$ . These studies, detailed in [13], revealed that the current pulse for the diodes readout should be kept to a width lower than 1 second to avoid self-heating effects. Therefore, the current pulse adopted for the study of the BPW34F radiation response was set to 1 mA  $\times$  700 ms. A reliable set of forward voltage growth curves has been then determined during irradiations carried out in different particle beams.

## V.FORWARD-BIAS DEVICE CALIBRATION IN HADRON FIELDS

Fig. 8 summarizes the increase of  $V_F$  versus the  $\Phi_{\text{eq}}$  recorded during different proton irradiation runs in IRRAD1 and IRRAD2 at CERN. The hardness factor values used to scale the CERN data plotted in Fig. 8 are the ones previously given in Sec. II.B. The proton data, obtained over two orders of magnitude of particle flux, don't reveal any significant rate effect. In the same plot the sensitivity to  $\gamma$ -rays has also been reported with cross markers. For the gamma irradiation, four

diodes were exposed at increasing doses from a  $^{60}\text{Co}$  source [19]. The four samples were exposed to TID of 0.1, 2, 10 and 22.6 kGy respectively as indicated in Fig. 8. The conversion between dose and photon fluence was obtained using the KERMA factor for 1.3 MeV photons in Silicon equal to 4.45 pGy·cm $^2$  [20]. Finally, in this summary plot, the results of two independent irradiations carried out with 0.8 MeV neutrons [21] and in the broad neutron spectrum of the TRIGA reactor at JSI [22] have also been included. For the first data set a direct calibration in terms of 1-MeV neutron equivalent fluence is available [23]. For the TRIGA reactor, both theoretical [24] and experimental [25] hardness factor are in very good agreement and equal to 0.90. All data presented in Fig. 8 have been measured at room temperature.

By fitting all different data set, it is possible to determine the calibration factor  $1/c$  of the linear relationship that links the growth of the forward voltage with the 1-MeV neutron equivalent fluence ( $\Delta V_F = c \cdot \Phi_{\text{eq}}$ ), so that:

$$1/c = 9.1 \times 10^9 \text{ cm}^{-2}/\text{mV} \quad (3)$$

The best fit of the data is in agreement within  $\pm 20\%$  with respect to the measured experimental data. The spread between the different data sets has probable origin in the errors that affects both the dosimetry measurements carried out in the irradiation facilities and the hardness factors that were used to normalize the different particle fluences. The agreement of the experimental data, the absence of rate-effects and the insensitivity to  $\gamma$ -rays proves the suitability of the BPW34F diode for the monitoring of the high particle fluences of interest for the LHC.

## VI. LONG-TERM ANNEALING AND TEMPERATURE DEPENDENCE

As mentioned in Sec. II.B, preliminary annealing tests performed on the BPW34F device showed that over 1 week the signal of the irradiated diodes decreases by about 25%. The long-term annealing of these devices has therefore been considered as an issue to be studied in detail to guarantee reliable measurements in long time monitoring applications.

Since the devices are surrounded by a plastic packaging, the effect of this package on the thermal behavior of the BPW34F diode has been investigated. For this purpose, one unirradiated device has been used as thermometer and heated up in different experimental conditions [13]. The temperature variation of the forward voltage upon 10  $\mu\text{A}$  current injection has been chosen as figure of merit. The first experiment consisted in heating up the diode by placing it in contact with a metal plate at a given temperature ranging from 70°C to 100°C. In such conditions, the forward voltage of the DUT stabilized at a given  $T$  after 10-100 min. from the beginning of the heating procedure. This long period needed to reach the thermal equilibrium clearly indicates that the thermal exchange between the device (e.g. silicon die) and the oven needs to be improved to allow precise annealing studies.

Therefore a second experiment was carried out by heating

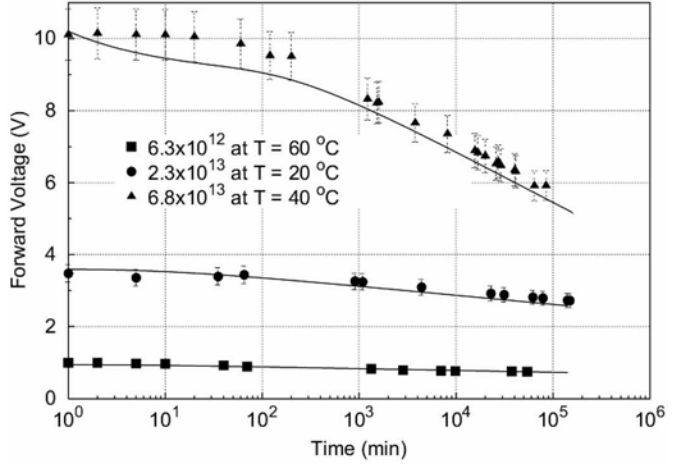


Fig. 9. Validation of the annealing parameterization for the BPW34F diodes.

up the DUT at the desired temperature in a volume of warm water. In this second case the thermal equilibrium was reached much faster: from 5 to 10 seconds after the beginning of the thermal cycle.

These preliminary measurements were used to establish the annealing protocol used in this work. In more detail, the measurement procedure consisted of three phases:

- to dip the diode in water at the selected annealing temperature over the desired annealing time;
- to quickly cool the diode down in water with melting ice for 10 seconds;
- to keep the diode in contact with a copper plate for 1 minute in order to get back to room temperature before starting the diode readout.

A series of irradiated BPW34F diodes has been exposed to this annealing procedure over a period of about 3 months in order to characterize the annealing dependence of the forward voltage as function of  $T$  and the  $\Phi_{\text{eq}}$ . The BPW34F samples used for this study were irradiated with protons at  $\Phi_{\text{eq}}$  ranging from  $2 \times 10^{12} \text{ cm}^{-2}$  to about  $1 \times 10^{14} \text{ cm}^{-2}$  and they were annealed at three selected temperatures (20, 40 and 60°C) with the above described procedure. The  $V_F$  readout during the annealing experiments was the same as established for the response curves of Fig. 8 (see Sec. V).

In analogy to what has been done for the leakage current related damage rate in silicon particle detector structures [25], [26], the long-term annealing of the forward voltage for the BPW34F diodes seems to follow a logarithmic function of the time. Thus the annealing of  $V_F$  at room temperature, as well as at higher temperatures, was chosen to be described by one exponential and a logarithmic term. Finally, in the same annealing function the temperature dependence of  $V_F$  has been also introduced so that:

$$V_F(t) = A - (|T_c| \times \Delta T) - \alpha \cdot \exp\left(\frac{t}{\tau}\right) - \beta \cdot \ln\left(\frac{t}{t_0}\right) \quad (4)$$

where,  $\Delta T = T - T_{\text{ref}}$  and the time was expressed in seconds. For each  $T$ , and for each  $\Phi_{\text{eq}}$ , the data were fitted

according to Eq. 4 with  $t_0$  set equal to 1 and  $T_{\text{ref}} = 20^\circ\text{C}$ . The temperature coefficient ( $T_c$ ) used in Eq. 4 has been instead measured from different set of diodes irradiated and annealed over long time-periods in various conditions.

The  $T_c$  for the BPW34F diodes is a negative value and it is function of  $\Phi_{\text{eq}}$ . Its value before irradiation is of  $-2.3 \text{ mV}^\circ\text{C}$ . The  $\Phi_{\text{eq}}$  dependence of this parameter can be fitted with the following linear function:

$$|T_c| = 8.3 \times 10^{-13} \cdot \Phi_{\text{eq}} + 2.3 \text{ mV}^\circ\text{C} \quad (5)$$

The other parameters  $A$ ,  $\alpha$  (amplitude of the exponential term), and  $\beta$  present in Eq. 4 have been found to be temperature independent, while their  $\Phi_{\text{eq}}$  dependence is rather complex and can be described by first and second order relations (see Appendix).

Finally, the Arrhenius plot of the time constant  $\tau$  revealed that:

$$\frac{1}{\tau} = k \cdot \exp\left(-\frac{E_A}{k_b \cdot T}\right) \quad (6)$$

where  $E_A$  and  $k$  are again dependent on  $\Phi_{\text{eq}}$  as shown in the Appendix. It has to be noted that the given parameterization holds only for the 3 months annealing time, for temperatures ranging from  $20^\circ\text{C}$  to  $60^\circ\text{C}$  and in the  $\Phi_{\text{eq}}$  range from  $2 \times 10^{12} \text{ cm}^{-2}$  to  $1 \times 10^{14} \text{ cm}^{-2}$ . The validity of the above parameterization has been finally tested on a series of devices irradiated in the same conditions with respect to the ones used for the parameterization.

As shown in Fig. 9, the calculation is in agreement better than  $\pm 10\%$  with respect to the experimental data sets measured in the above mentioned temperature and fluence range. Therefore, in operative conditions when the measurements extend on a monthly scale Eq. 4 can be implemented, within an iterative procedure, in order to correct the signal read out from the BPW34F devices.

In the investigated temperature range the annealing has the following behavior: for the first 100 minutes the dosimetric signal shows only a small degradation. For  $t$  greater than 100 minutes the degradation speed increases and the loss reaches about 40% over more than 2 months at the maximum  $\Phi_{\text{eq}}$  considered in this study. In the investigated annealing time, evidences of saturation phenomena have not been observed. This finding suggests a repeated experiment with experimental data that span over a wider time interval.

## VII. CONCLUSION

To provide the LHC experiments with  $p\text{-}i\text{-}n$  diode sensors with a broad measurement range, the OSRAM BPW34F commercial diodes powered at 1 mA are a valuable choice since they allow measurements over a high-fluence range with a good sensitivity.

As proven in this work, the radiation-induced modifications of the diode parameters have been understood and its particle-sensitivity has been measured with good accuracy in various

experimental conditions. In particular, an explanation of the modifications of the diode's I/V characteristic due to heavy hadron irradiation has been given.

The calibration curves presented here reveal that the BPW34F device is not sensitive at  $\Phi_{\text{eq}}$  levels  $< 2 \times 10^{12} \text{ cm}^{-2}$ . A sensitivity of  $9.1 \times 10^9 \text{ cm}^{-2}/\text{mV} \pm 20\%$  has been obtained for higher fluence levels.

The long-term annealing of the  $\Delta V_F$  has been identified as the limiting factor for such devices. For this reason an experimental parameterization to correct the time behavior of  $\Delta V_F$  as function of the operational  $T$  and the cumulated  $\Phi_{\text{eq}}$  has been proposed in this work.

As proposed [2] and verified elsewhere [27], a complete monitoring of the 1-MeV neutron equivalent fluence in accelerator environment, like the one encountered in the Experiments of the CERN LHC, can be achieved complementing the BPW34 devices by using high-sensitivity  $p\text{-}i\text{-}n$  diodes. However, the BPW34 diodes can be brought immediately to their operation point, by performing pre-irradiation to a  $\Phi_{\text{eq}}$  level of  $2 \times 10^{12} \text{ cm}^{-2}$ . This pre irradiation step is not followed by annealing as shown in [13]. In this way the initial "insensitive" region recorded in the device's radiation response (see Fig. 8) can be eliminated without altering its sensitivity for the higher fluence range as it has been shown in our previous work [28].

## APPENDIX

The parameters  $A$ ,  $\alpha$  and  $\beta$  of Eq. 4 follow linear relationships of the form:

$$X = x_1 \cdot \Phi_{\text{eq}}^2 + x_2 \cdot \Phi_{\text{eq}} + x_3 \quad [\text{V}]$$

Where the experimental coefficients  $x_i$  are given here in the below Table II:

The coefficients of Eq. 6 have the form:

$$\begin{aligned} E_A &= 0.236 \cdot \exp(1.97 \times 10^{-14} \cdot \Phi_{\text{eq}}) \quad [\text{eV}] \\ k &= 1.706 \cdot \exp(3.27 \times 10^{-13} \cdot \Phi_{\text{eq}}) \quad [\text{s}^{-1}] \end{aligned}$$

## ACKNOWLEDGMENT

The authors acknowledge colleagues who have provided radiation sources and performed irradiations of the studied devices, including E. Dimovasili from CERN for the gamma irradiation and I. Mandic from the Jozef Stefan Institute of Ljubljana, Slovenia for neutron irradiations.

TABLE II  
FLUENCE DEPENDENCE OF THE LONG-TERM ANNEALING PARAMETERS

Parameter	$x_1$	$x_2$	$x_3$
$A$	0	$1.09 \times 10^{-13}$	-0.46
$\alpha$	$4.23 \times 10^{-28}$	$4.51 \times 10^{-15}$	0.051
$\beta$	$9.66 \times 10^{-29}$	$2.42 \times 10^{-15}$	0.003

## REFERENCES

- [1] The Large Hadron Collider Technical Design Report, vol. 1-4. CERN-2004-003, 2004.
- [2] F. Ravotti, M. Glaser, M. Moll, K. Idri, J.-R. Vaillé, H. Prevost, and L. Dusseau, "Conception of an integrated sensor for the radiation monitoring of the CMS experiment at the large hadron collider," *IEEE Trans. Nucl. Sci.*, vol. 51, no. 6, pt. 2, pp. 3642–3648, Dec. 2004.
- [3] R. K. Bock and A. Vasilescu, "The Particle Detector Brief Book", Springer-Verlag Berlin Heidelberg, 1998 (for more details see also ROSE/TN/97-2 available on <http://www.cern.ch/rd48/> and the "displacement damage in silicon on-line compilation" available on <http://sesam.desy.de/members/gunnar/Si-dfunes.html>).
- [4] BPW34 silicon p-i-n photodiode Datasheet [Online]. Available from OSRAM Opto-Semiconductors: <http://www.osram-os.com>.
- [5] M. Tavlet, M. E. Leon Florian, "PSAIF: the PS-ACOL irradiation facility at CERN," In. Proc. of First European Conference on Radiation and its Effects on Devices and Systems, RADECS 91, La Grand Motte, 9-12 Sept. 1991, pp. 582 – 585.
- [6] L. Malfante, "Utilisation de dosimètres semi-conducteurs au silicium autour des accélérateurs de particules à haute énergie," CERN-TIS-CFM/IR/92-09, 1992.
- [7] M. Glaser, F. Ravotti and M. Moll, "Dosimetry Assessments in the Irradiation Facilities at the CERN-PS Accelerator," *IEEE Trans. Nucl. Sci.*, vol. 53, pp. 2016-2022, 2006.
- [8] M. Moll, E. Fretwurst, M. Kuhnke, and G. Lindström, "Relation between microscopic defects and macroscopic changes in silicon detector properties after hadron irradiation," *Nucl. Inst. and Meth.*, vol. B186, pp. 100–110, 2002.
- [9] M. Huhtinen, Recommendations for irradiations of CMS components in the IRRAD2 facility at PS, CERN, CMS-IN-2001-012, 2001.
- [10] M. Swartz, M. Thurston, "Analysis of effect of fast-neutron bombardment on the current-voltage characteristic of conductivity modulated p-i-n diodes," *J. Appl. Phys.*, vol. 37, no. 2, pp. 745-755, 1966.
- [11] A. Rosenfeld et al., "p-i-n diodes with a wide measurements range of fast neutron dose," *Rad. Prot. Dos.*, vol. 33(1-4), pp.175-178, 1990.
- [12] G.Lindström et al., "Developments for radiation hard silicon detectors by defect engineering – results by the CERN RD48 (ROSE) Collaboration," *Nucl. Instr. and Meth.*, vol. A 465, pp. 60-69, 2001.
- [13] F. Ravotti, "Development and characterization of radiation monitoring sensors for the high energy physics experiments of the CERN LHC Accelerator (Thesis)", Ph.D. dissertation, Department of Electronics, University Montpellier II, Montpellier, France, 2006. Also in CERN Thesis collection CERN-THESIS-2007-013.
- [14] D. K. Schroder, "Semiconductor Material and Device Characterization", John Wiley & Sons, 1990, ISBN 0-471-51104-8.
- [15] A. G. Holmes-Siedle and L. Adams, Handbook of Radiation Effects, 2nd ed. Oxford, U.K.: Oxford University Press, 2002.
- [16] E. Fretwurst, H. Feick, M. Glaser, et al., "Reverse annealing of the effective impurity concentration and long term operational scenario for silicon detectors in future collider experiments," *Nucl. Inst. and Meth.*, vol. A342, pp. 119–125, 1994.
- [17] S. J. Bates, B. Dezillie, C. Furetta, M. Glaser, F. Lemeilleur, E. Leon-Florian, "Proton irradiation of various resistivity silicon detectors," *IEEE Trans. Nucl. Sci.*, vol. 43, pp. 1002-1008, 1996.
- [18] E. Lorfevre et al. "Heavy ion induced failures in a power IGBT", *IEEE Trans. Nucl. Sci.*, vol. 44, pp. 2353-2357, Dec. 1997.
- [19] E. Dimovasili, "Total Dose Tests of Technical Equipment for the LHC", Presentation given at the 5<sup>th</sup> LHC RADIATION WORKSHOP, CERN 29 November 2005. Available online: <http://www.cern.ch/lhc-radwg>.
- [20] J. H. Hubbell, "Photon mass attenuation and energy absorption coefficients from 1 keV to 20 MeV," *Int. J. Appl. Radiat. Isot.*, vol. 33, pp. 1269–1290, 1982.
- [21] T. Wijnands. Interfacing with the LHC accelerator during physics operation. Proc. 11th LECC Workshop, Heidelberg, Germany, TS-Note-2005-054, 2005.
- [22] G. Kramberger. Development of ATLAS Radiation Monitor, Presentation given at the CERN RADMON meeting 16 November 2004.
- [23] J. Morin, P. Zyromski, "The PROSPERO and CALIBAN neutron irradiation facilities", In. Proc. of First European Conference on Radiation and its Effects on Devices and Systems, RADECS 91, La Grand Motte, 9-12 Sept. 1991, pp. 574 – 576.
- [24] D. Zontar, "Study of radiation damage in silicon detectors for high luminosity experiments at LHC (Thesis)" - PhD dissertation, Ljubljana, Slovenia, 1989.
- [25] M. Moll, "Radiation damage in silicon particle detectors - Microscopic defects and macroscopic properties (Thesis)" - PhD dissertation, University of Hamburg, Germany, 1999. DESY-THESIS-1999-040, ISSN 1435-8085.
- [26] M. Moll et al., "Leakage current of hadron irradiated silicon detectors – material dependence," *Nucl. Instr. and Meth.*, vol. A 426, pp 87-93, 1999.
- [27] F. Ravotti, M. Glaser, A.B. Rosenfeld, M.L.F. Lerch, A.G. Holmes-Siedle and G. Sarrabayrouse, "Radiation Monitoring in Mixed Environments at CERN: from the IRRAD6 Facility to the LHC Experiments," *IEEE Trans. Nucl. Sci.*, vol. 53, no. 4, pp. 1170-1177, 2007.
- [28] F. Ravotti, M. Glaser and M. Moll, "SENSOR CATALOGUE – Data compilation of solid-state sensors for radiation monitoring," CERN TS Tech. Note, TS-Note-2005-002, 2005.